Experimental and Numerical Investigation of the Condensed Combustion Products of AP-based Rocket Propellants

S. Cerri, G. Gariani*, F. Maggi*, A. Bandera*, L. Galfetti*, L. T. DeLuca*, F. Lillo**, and V. Babuk****
**SPLab, Dipartimento di Energetica, Politecnico di Milano, I –20156 Milan, Italy*
***Avio S.p.A., I-00034 Colleferro, Rome, Italy*
****Baltic State Technical University, 190005 Saint Petersburg, Russia*

Abstract

Four industrial AP-based, aluminized propellants were tested to characterize agglomeration phenomena and the condensed combustion products (agglomerates and micrometric oxide particles). Aggregation/agglomeration phenomena were investigated with a High Speed and High Resolution video system. Condensed combustion products were analyzed with advanced techniques (Scanning Electron Microscopy, X-Ray Photoelectron Spectroscopy and X-Ray Diffraction) to determine morphology, chemical composition and crystalline structure. A numerical investigation on condensed combustion products evolution in the combustion chamber was started. Preliminary results, concerning very specific aspects of the approach are presented.

Nomenclature

Al^0 = metallic aluminum
Al_2O_3 = alumina
Al_{ox} = aluminum oxide
AP = Ammonium Perchlorate
HTPB = Hydroxyl-Terminated Polybutadiene
XPS = X-Ray Photoelectron Spectroscopy
XRD = X-Ray Diffraction
SEM = Scanning Electron Microscopy
MOPs = Micrometric Oxide Particles
CCPs = Condensed Combustion Products
SOPs = Smoke Oxide Particles

1. Introduction

Metals, particularly aluminum powders, are inserted into propellants formulation with the purpose of increasing the energetic performance. During combustion processes aluminum undergoes a series of chemical-physical phenomena leading to the formation of condensed combustion products (CCPs). Combustion processes are divided in two stages. The first one is related to the condensed phase of the burning propellant where the key phenomenon is agglomeration, the second one is the two-phase flow in the combustion chamber[1]. Metal particles are retained, move and coalescence on the burning surface involving different pocket mechanisms: pockets, inter-pockets bridges and prior-to-pockets[1,2]. Skeleton layer is the necessary condition for agglomerates formation; this is a three-dimensional structure consisting of metal, oxide and carbonaceous elements. It only occurs within pockets and characterizes the upper part of the propellant burning surface (carbon skeleton)[2,3]. Residuals populations contain particles derived from not agglomerating aluminum powders, intermediate and pocket-size agglomerates, large inter-pocket agglomerates and smaller products[4]. Russian literature usually classifies CCPs in agglomerates ($D > 30$ μm) and smoke oxide particles (SOPs) ($D < 30$ μm)[2-3], or agglomerates ($D > 30$~60 μm), micrometric oxide particles (MOPs) (1~2 μm < $D < 30$~60 μm), and SOPs ($D < 1$~2 μm)[5]. Micrometric oxide particles come from the transformation of oxide cap on

each Al particle during combustion into a single oxide particle after full aluminum consumption[5]. The agglomerate structure generally is divided in two concepts: agglomerates are only made of aluminum unburned (Al^0) and alumina (Al_2O_3), or agglomerates are constituted of Al^0, Al_2O_3 and other elements (not necessary of spherical shape)[1]. The characteristics of agglomerates and MOPs is important because these particles affect and control the stability of the rocket motor. Oxide particles can provide efficient damping pressure oscillations ; smoke oxide particles are able in damping high frequency oscillations (above 4000 Hz) and larger residuals oxide particles are effective in damping low and middle frequency oscillations[6].

This work is focused on the characterization of agglomerates and micrometric oxide particles formed near the combustion surface[7]. Agglomerates are considered constituted only of Al^0 and Al_2O_3. The first part of the paper shows solid propellants formulations; then the attention is focused on the aggregation/agglomeration phenomena through the analyses of visualization frames. Information about the mean agglomerates diameter and agglomerates histograms at different pressure levels is obtained. In the last part CCPs are investigated with analytical techniques: agglomerates morphology is evidenced with Scanning Electron Microscopy (SEM) analysis; CCPs surface chemical composition is investigated with X-Ray Scanning Photoelectron Spectroscopy (XPS) and finally crystallographic structure is studied with X-Ray Diffraction technique (XRD). This experimental investigation of the agglomeration phenomena supports the validation of metallized solid rocket propellants combustion models. A numerical investigation strategy and preliminary numerical results are proposed with the purpose to better understand the agglomerate evolution. Concluding remarks and future developments complete the paper.

2. Solid propellant formulations

Composite solid propellants tested were industrial products. The composition is proprietary but general characteristics are given in Table 1. Three propellants with the same ammonium perchlorate, aluminum and polymeric binder (AP/Al/HTPB) nominal composition but different powder sizes were investigated together with a common 68/18/14 propellant taken as reference one. All propellants contain bi or three-modal oxidizer grains. Reference and D propellants are quite similar; propellants B and C differ only for the AP coarse amount (B contains a greater amount of 200 μm respect to 400 μm, and propellant C is the opposite).

Table 1 : AP grain size distribution and density

	Reference	**B**	**C**	**D**
AP size distribution	Fine[a], 200	Fine, 200, 400	Fine, 200, 400	Fine, 200
AP qualitative fine amount	High	Low	Medium	High
$<\rho>$	1.729	1.788	1.779	1.775

[a] Fine AP means AP particles size of the order of 10 μm.

Propellants were analyzed to evaluate aggregation/agglomeration phenomena and to characterize the condensed combustion products in term of morphology, size, chemical composition and structure.

3. Visualization of the aggregation/agglomeration phenomena

The purpose of the visualization analyses was the characterization of the growth mechanism of the condensed combustion products and the evaluation of the mean diameter of the condensed particles leaving the burning surface. The visualization of aggregates dynamics, first, and conversion to agglomerates, then, aimed at understanding the details of burning surface phenomena. A qualitative information was obtained through the comparison of the agglomeration process featured by different propellants.

Cuts of 4x4x20 mm were taken from the original industrial material only after a period of acclimation (at least 12 hours of conditioning at ambient temperature). Samples were laterally inhibited and burned only after another period of 12 hours.

Combustion tests at 5, 10, 20, and 25 bar were performed in a horizontal combustion chamber with optical accesses. Ignition was performed by a single laser pulse; pressure was maintained at a constant value, during the whole combustion process, by an automatic control system; combustion was performed in nitrogen atmosphere. A simple scheme of the experimental line is reported in Figure 1.

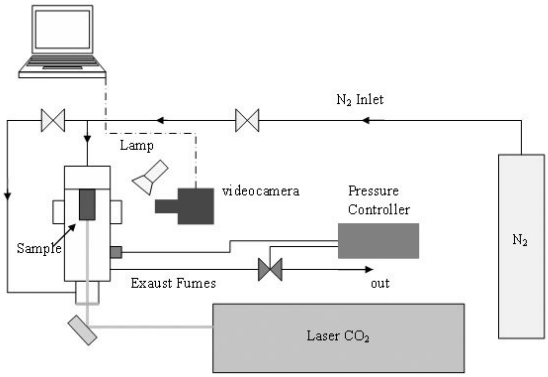

Figure 1 : Combustion chamber for the study of the aggregation/agglomeration phenomena

Recording of tests was performed with a High Speed and High Resolution video system with a long-range microscope; the light was given by a cold-light source. Video camera was focused at about 5 mm from the beginning of the sample in order to exclude the burning transient and to record steady-state combustion. Calibration of dimensions was performed and repeated several times for each test session.
From the analysis of visualization frames it was possible to measure the characteristic dimensions and the diameter of condensed products leaving the burning surface (agglomerates had a characteristic spherical shape). Any agglomerate is subjected to a strong redox reaction on its surface just after detachment. This causes the agglomerate to heat up and increase luminosity with the consequence of enlarging its apparent dimension on the camera sensor. The measurement of one particle just before the detachment can give an estimate reasonably closer to the real value. This kind of analysis allows only a qualitative comparison between different formulations because of the limited number of sampling done for each movie (100-150). The technique is also subjected to operator sensitivity. Hence, these data have a probabilistic feature, unlike residues collection that gives a statistical analysis of the condensed combustion products (see next session). Nevertheless, the technique permitted to gather some information about agglomerates during the detachment phase. Figure 2 shows the sequence of the agglomeration phenomena. In the first phase the agglomerates exist only as aggregates of irregular shape ("cluster" of elongated shape[8]), then through the progressive heating particles melt and coalescence to form a single drop with the characteristic round shape[5]. After this step the agglomerate (metal and oxide cap) keeps on growing until the detachment instant.

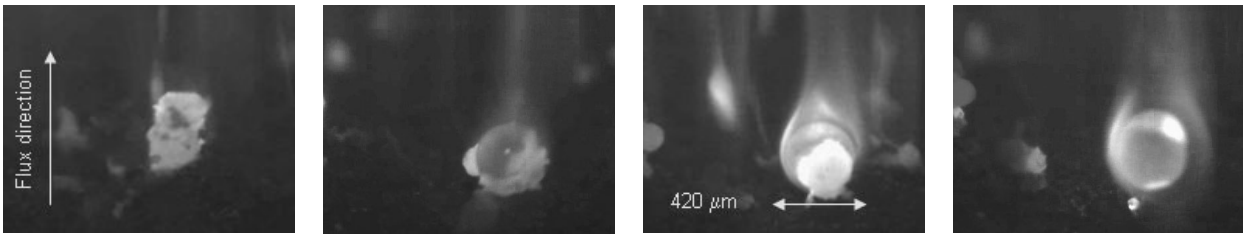

Figure 2 : Agglomeration sequence of Reference propellant (p = 5 bar, 2000 fps, nominal magnification 3x)

Movies were analyzed with a dedicated software and decomposed frame by frame. At least 100 measures were realized for each test conditions. Histograms were obtained for each testing condition. 20 equally spaced intervals were considered. Figure 3a evidences a typical histogram.

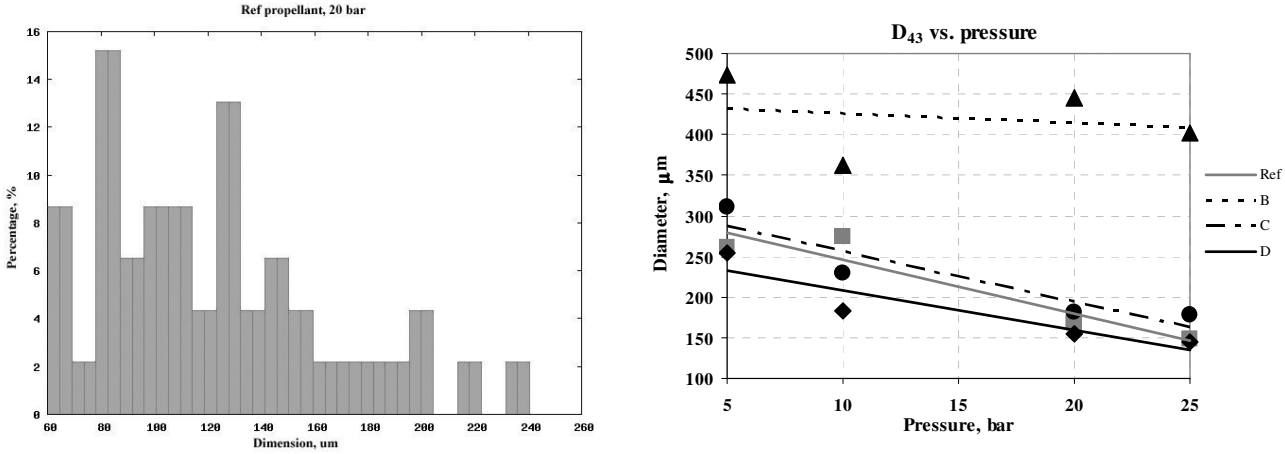

a b

Figure 3

a: Histogram of Reference propellant burned at 20 bar b: D_{43} at different pressures

Figure 3b presents the diameter D_{43} of different propellants tested at 4 pressure values. Propellant B generates large agglomerates, propellant D was comparable with the reference propellant; propellant C showed an intermediate behavior.

4. CCPs analysis

Propellants were tested at 10, 20 and 30 bar. Samples (4.5x4.5x30 mm) were inhibited on the sides and then dried for more than 24 hours at ambient temperature. A sketch of the combustion chamber used to collect CCPs is shown in Figure 4. Condensed combustion residues were collected into the inert liquid and then they were thermally conditioned at 50 °C in order to evaporate the liquid fraction. Then they were analyzed.

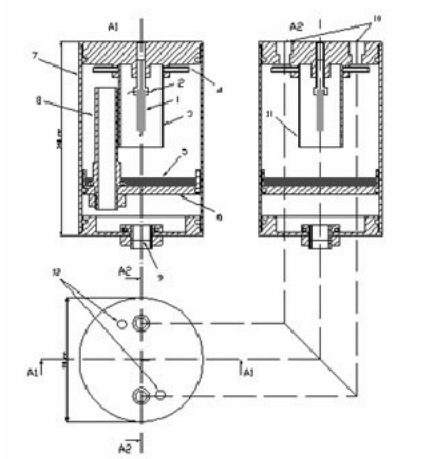

1. Propellant sample
2. Pin propellant sample
3. Confinement cylinder
4. Screws between head of combustion chamber and confinement cylinder
5. Quenching liquid
6. Quenching pool
7. Central stainless steel cylinder
8. Link cylinder between collecting chamber and transit chamber
9. Cellulose filters
10. Openings for igniter system
11. Openings for Ni-Cr wire
12. Openings for screws of test chamber

Figure 4 : Sketch of the combustion chamber used to collect residues

Different kinds of analyses required a great amount of materials so for every experimental point at least 5 propellants samples were burned and the average value extracted. All experiments were performed under identical operating conditions (pressure, temperature, sample preparation, lateral surface inhibition, and ignition technique) to guarantee the results reproducibility[9].

4.1 SEM analysis

SEM analysis gives information about the morphology of the combustion residues (see details in[10]). Examples of SEM combustion residues micrographs, collected at 10 and 30 bar, are shown in Figure 5. Micrographs show the complex morphology of these materials. It was also possible to identify alumina particles thanks to their spherical shape (agglomerate shape is controlled by the surface tension of its main constitutive elements, Al^0 and Al_2O_3, both in a liquid state)[1]. Moreover the presence of SOPs and MOPs was observed. The general trend shown by SEM analyses seems to confirm, for the industrial propellants investigated in this work, that aggregation/agglomeration phenomena are higher for propellants containing larger oxidizer particles.

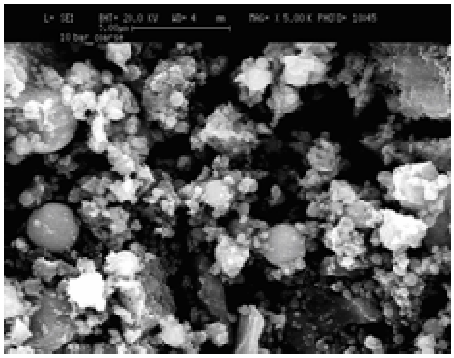

(Reference propellant, 10 bar, magnification 5kx)

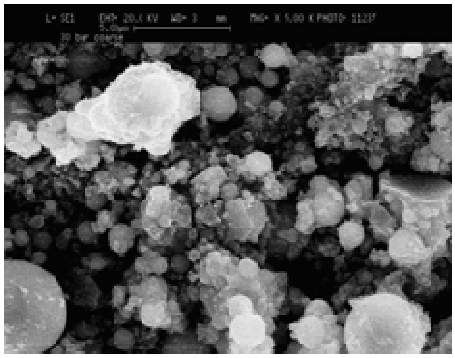

(Reference propellant, 30 bar, magnification 5kx)

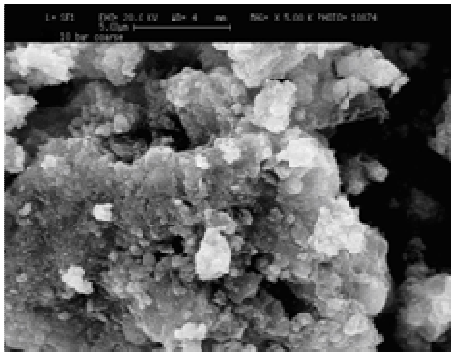

(B propellant, 10 bar, magnification 5kx)

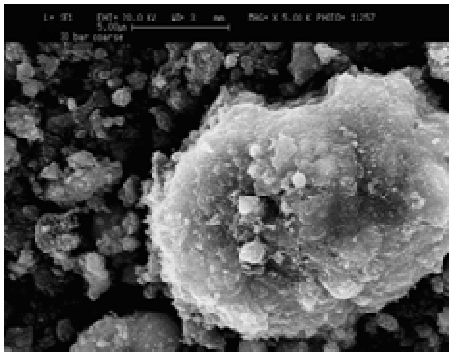

(B propellant, 30 bar, magnification 5kx)

Figure 5 : SEM micrographs of Reference and B propellants burned at 10 and 30 bar

4.2 XPS analysis

X-Ray Photoelectron Spectroscopy was used to measure the surface atomic concentration of the chemical elements (see details in[10,11]). XPS analyses focused the attention only on the CCPs surface while bulk composition was investigated by XRD. Data from XPS analysis represent an average result of the sampled zone that usually contains a great amount of particles (CCPs, MOPs and SOPs). XPS analyses are local, but the heterogeneity of material is representative of what occurred during the combustion processes. Table 2 shows the total amount of atomic species for each propellant burned at 30 bar. Particular attention was given to aluminum, carbon, and chlorine content. Formulations containing large oxidizer grains gave greater amount of carbon content due to an incomplete decomposition process of binder (part of this carbon was oxidized). Chlorine is probably chlorine derived from an incomplete decomposition of the oxidizer grains as well. Aluminum was the total Al, mainly detected as aluminum oxide (Al_{ox}), in fact Al^0, contained inside CCPs, does not appear in a surface analysis.

Table 2 : Surface chemical composition of CCPs (30 bar)

	Reference	**B**	**C**	**D**
C1s, at%	32.3	45.5	40.2	35.9
O1s, at%	34.3	26.3	27.9	31.9
Al2p, at%	23.3	16.6	12.9	20.8
Cl2p, at%	5.8	9.4	6.1	6.3
Other, at%	4.2	2.2	12.9	5.0

4.3 XRD analysis

XRD spectra were obtained with a computer controlled diffractometer (see details in[10,11]). Crystalline phases and their relative abundance were obtained trough XRD spectra. Qualitative analysis has been carried out by the Hanawalt search method on the data set PDF-2 (Powder Diffraction File, ICDD[12]). Quantitative analysis has been obtained with the use of Rietveld method.

Combustion residues evidence the presence of four kinds of alumina: α-Al_2O_3 (stable phase, also called Corundum), δ-Al_2O_3, δ*-Al_2O_3, γ-Al_2O_3. The sum of these four phases (three were metastable transition phases) compared to the unburned aluminum amount, Al^0, gave a quantitative comparison among different formulations. Table 3 evidences the phases contained into CCPs. The unburned aluminum content (Al^0) suggests that a higher pressure favor the combustion process and the aluminum combustion[13]. This is true for all propellants except for propellant B: a higher pressure did not favor the combustion process. The aluminum powders, especially the larger aluminum agglomerates, did not have enough time to complete the oxidation process (quenching pool was always maintained at the same average distance from the sample burning surface) so a great amount of metal unburned remained in the condensed combustion products.

Table 3 : Crystal phases of CCPs (10 and 30 bar)

	Reference		**B**		**C**		**D**	
	10 bar	30 bar	10 bar	30 bar	10 bar	30 bar	10 bar	30 bar
Al^0, %	17.7	13.4	19.0	28.5	31.4	14.8	22.7	8.8
γ-Al_2O_3, %	34.2	35.6	37.8	34.2	35.4	38.2	37.1	40.5
δ-Al_2O_3, %	10.0	23.3	2.8	4.1	5.6	10.9	10.0	22.6
δ*-Al_2O_3, %	24.9	24.8	28.8	21.8	24.6	27.2	23.2	22.2
α-Al_2O_3, %	12.7	2.9	7.2	8.2	3.0	7.6	6.4	5.7
Other	0.5	traces	4.4	3.2	traces	1.3	0.6	0.2

5. Numerical investigation

The knowledge and modeling[14] of CCPs behavior in the combustion chamber of a solid rocket represents a fundamental step for the motor design. The general strategy of this group to model the CCPs behavior, originated by the combustion of metallized solid propellants, includes the following steps:

1. to develop a model for the formation of agglomerates at the propellant burning surface, their evolution and their detachment from the surface;
2. to model the effects of gaseous combustion products on agglomerates burning process;
3. to model the details of the metal burning;
4. to model the chemical interaction between metal and its oxides, which affect the agglomerate structure.

Two examples are presented to show preliminary simulations of specific effects in the framework of the described numerical approach.

The first concerns the fluid-dynamic field and the heat transfer around three spherical aluminum particles, whose diameters are assumed to be 0.5, 1.0 and 1.5 mm respectively, invested by a cold air flow (constant properties, evaluated at 290 K) at three different velocities: 1 m/s (Re = 2733, laminar flow), 2.5 m/s (Re = 6000, immediately after transition), and 10 m/s (Re = 27330, turbulent flow). Particles are still in a 2-D combustion chamber, 8 cm long and 4 cm high; the flow at the inlet has a parabolic shape. No-slip conditions are considered on the particles surface. Results are summarized in Figures 6-8. Figures 6 and 7 point out the flow field determined in laminar and turbulent regimes under isothermal conditions and Figure 9 shows recirculation regions typical of a fully developed turbulent flows, obtained at higher Reynolds number.

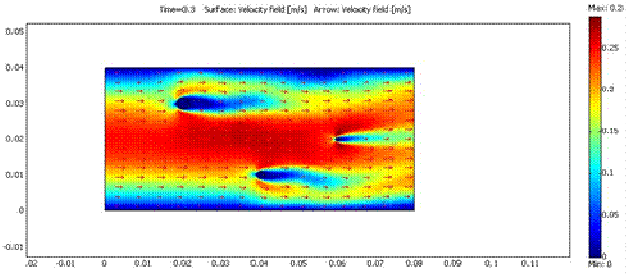

Figure 6 : Fluid-dynamic flow field in laminar regime. Inlet velocity: 1.0 m/s

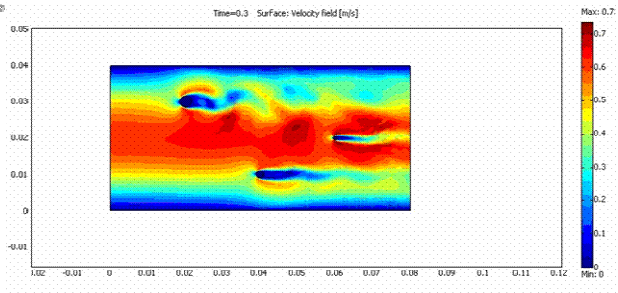

Figure 7 : Fluid-dynamic flow field in turbulent regime. Inlet velocity: 2.5 m/s

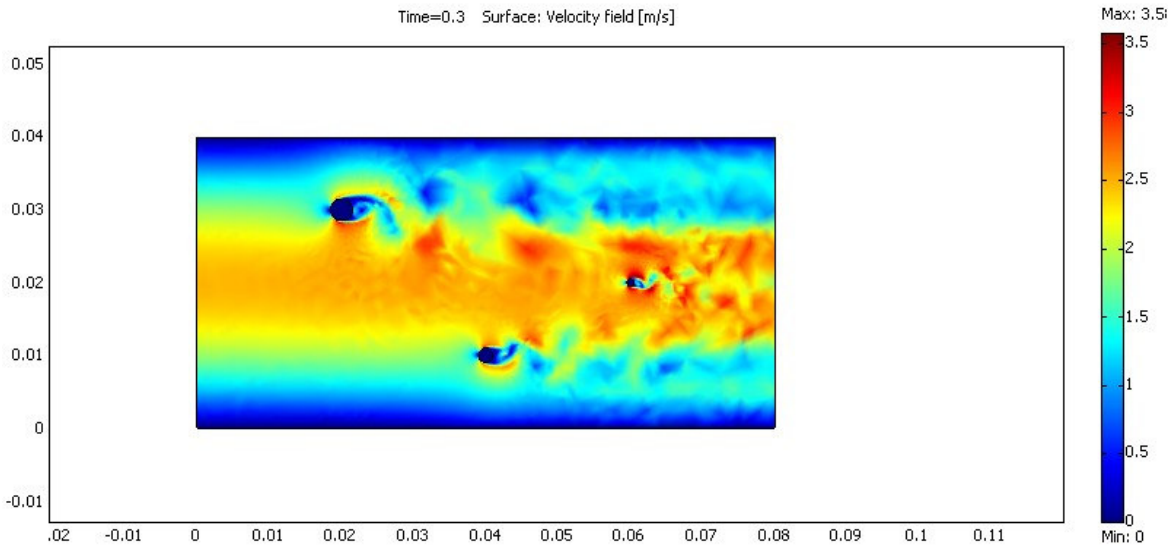

Figure 8 : Fluid-dynamic flow field in fully developed turbulent regime. Inlet velocity: 10 m/s

Numerical simulations were then performed considering heat transfer. Particles were assumed to be at 3000 K, and conductive and convective heat transfer with the surrounding atmosphere were considered. Results are presented in Figures 9-11, which show that the temperature gradient has the highest value in the stagnation region of the particles invested by the cold flow.

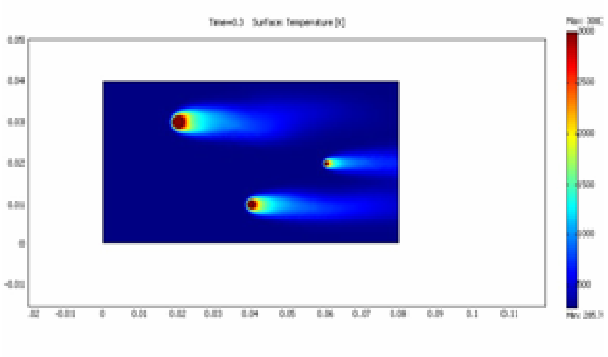

Figure 9 : Temperature distribution in laminar flow conditions. Inlet velocity: 1.0 m/s
Temperature particle: 3000 K
Temperature inlet flow: 290 K

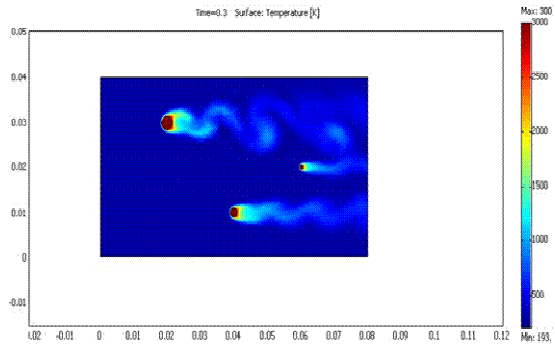

Figure 10 : Temperature distribution in laminar flow conditions. Inlet velocity: 2.5 m/s
Temperature particle: 3000 K
Temperature inlet flow: 290 K

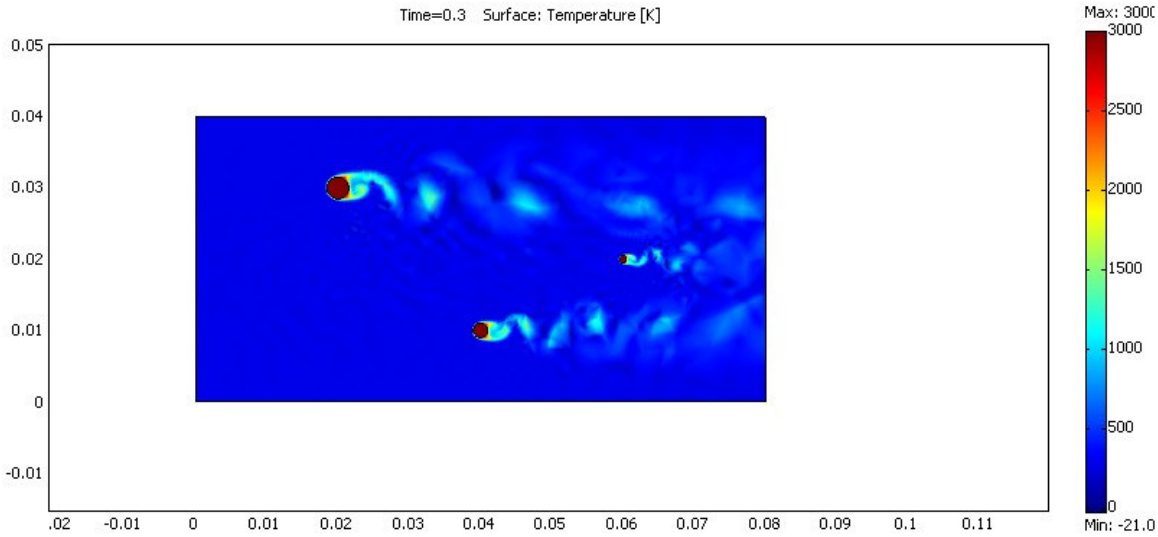

Figure 11 : Temperature distribution in fully developed turbulent regime. Inlet velocity: 10 m/s
Temperature particle: 3000 K. Temperature inlet flow: 290 K

A fixed regression rate of 0.5 mm/s, to simulate the particle evaporation, was then considered in order to test the moving boundary capability of the numerical code. Results of Figure 12 show the influence of the reduced surface on the fluid-dynamic field surrounding the droplet.

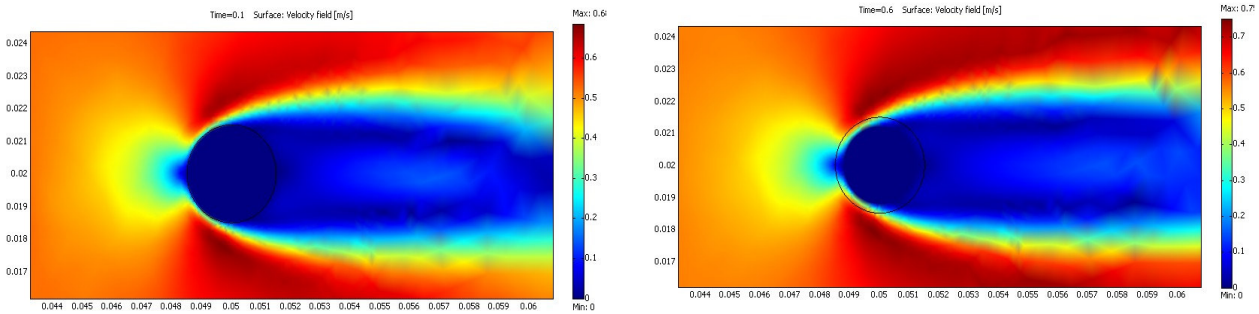

Figure 12 : Fluid dynamic field around an evaporating droplet

6. Conclusions

Four industrial, AP-based aluminized propellants were investigated in order to study the CCPs dependence on propellant formulation. High Speed and High Resolution video system techniques, SEM, XPS and XRD analyses allowed to characterize the condensed products, showing the important effects of the oxidizer grain size on aluminum agglomeration phenomena at the propellant burning surface. Large oxidizer grain sizes yield larger agglomeration. A mathematical modeling approach to study the evolution of agglomerates and condensed products was considered, and preliminary results concerning the interaction between solid particles and the fluid-dynamic field are presented.

7. Future work

Future work will be addressed to optimize the propellant formulation taking into account the results meanwhile obtained from the CCPs experimental analyses. According to the previously described numerical strategy, the numerical work will focus on the agglomerate regression rate determined by the metal combustion in an oxidizing atmosphere. The agglomerate will be considered constituted by a liquid fraction and a solid oxide fraction, changing in time and during the agglomerate evolution in the combustion chamber. The research activity will be addressed to the mathematical model development, in order to describe the complex phenomena experimentally observed.

References

[1] Babuk, V.A., Vasilyev, V.A. and Malakhov, M.S. Condensed combustion products at the burning surface of aluminized solid propellant, *Journal of Propulsion and Power*, Vol. 15, No. 6, pp. 783–793, 1999.
[2] Babuk, V.A., Vassiliev, V.A. and Sviridov, V.V., Propellant formulation factors and metal agglomeration in combustion of aluminized solid rocket propellant, *Combustion Sci. and Tech.*, pages 261–289, 2001.
[3] Babuk, V.A., Vassiliev, V.A. and Sviridov, V.V. Formation of condensed combustion products at the burning surface of solid rocket propellant, Solid Propellant Chemistry, Combustion and Motor Interior Ballistic, *Progress in Astronautics and Aeronautics*, edited by Yang V., Brill T.B., Ren W.Z., AIAA, 185: 749–776, 2000.
[4] Price, E.W. and Sigman, R.K. Combustion of aluminized solid propellants, Solid Propellant Chemistry, Combustion and Motor Interior Ballistic, *Progress in Astronautics and Aeronautics*, edited by Yang V., Brill T.B., Ren W.Z., AIAA, 185: 663–687, 2000.
[5] Glotov, O.G. and Zarko, V.E. Condensed combustion products of aluminized propellants, *Aeronautical and Astronautical Society of the Republic of China*, 34: 3: 247–256, 2002.
[6] Dokhan, A., Price, E.W., Sigman, R.K. and Seitzman, J.M. Combustion mechanism of bimodal and ultra-fine aluminum in AP solid propellant, *38th AIAA/ASME/SAE/ASEE Joint Propulsion Conference and Exhibit*, Indianapolis, IN, AIAA Paper 2002-4173, July 2002.
[7] Salita, M. Internal aerodynamics in solid rocket propulsion, von Karman Institute for Fluid Dynamics, RTO AVT/VKI Special Course, May 27-31, 2002.
[8] Grigor'ev, V.G., Zarko, V.E. and Kutsenogii, K.P. Experimental investigation of the agglomeration of aluminum particles in burning condensed systems, *Combustion, Explosion and Shoke Waves*, 17: 3: 245–250, 1981.
[9] Glotov, O.G, The Condensed Combustion Products of Aluminized Solid Propellants. II. Evolution of Particles with Distances from the Burning, *Combustion, Explosion and Shoke Waves*, 36: 4: 476–487, 2000.
[10] Galfetti, L., Severini, F., DeLuca, L.T., Marra, G., Meda, L. and Braglia, R. Ballistic and Condensed Combustion Residues of Aluminized Solid Rocket Propellants, *Proceedings of the 9-IWCP – The Ninth International Workshop on Combustion and Propulsion*, Novel Energetic Material and Applications, grafiche g.s.s., Bergamo, Italy, 2004, paper No.18.
[11] Galfetti, L., DeLuca, L.T., Severini, F., Cerri, S., Lentini, L., Meda, L., Marra, G. and Babuk, V.A. Experimental Investigation and Numerical Modeling of the Condensed Combustion Products of Micro and Nano-Aluminized Solid Propellants, IAC-06-C4.3.03, *International Astronautical Congress*, Valencia, Spain, 2-6 October 2006.
[12] ICDD, International Center for Diffraction Data, Pennsylvania, USA.
[13] Cerri, S. Experimental Investigation of the Condensed Combustion Residues of Aluminized Solid Rocket Propellants for Space Applications, Master Thesis in Aeronautical Engineering, Politecnico di Milano, SPLab, July 2006 (in Italian).
[14] Babuk, V.A., Vassiliev, V.A. Model of aluminum agglomerate evolution in combustion products of solid rocket propellant, *Journal of Propulsion and Power*, Vol. 18, No. 4, 2002.

This page has been purposedly left blank